Status of vibrational structure in ^{62}Ni

A. Chakraborty,[1,*] J. N. Orce,[1,†] S. F. Ashley,[1,‡] B. A. Brown,[2,3] B. P. Crider,[1] E. Elhami,[1,§] M. T. McEllistrem,[1] S. Mukhopadhyay,[1,‖] E. E. Peters,[4] B. Singh,[5] and S. W. Yates[1,4]

[1]*Department of Physics and Astronomy, University of Kentucky, Lexington, Kentucky 40506-0055, USA*
[2]*National Superconducting Cyclotron Laboratory, Michigan State University, East Lansing, Michigan 48824, USA*
[3]*Department of Physics and Astronomy, Michigan State University, East Lansing, Michigan 48824, USA*
[4]*Department of Chemistry, University of Kentucky, Lexington, Kentucky 40506-0055, USA*
[5]*Department of Physics and Astronomy, McMaster University, Hamilton, Ontario, Canada L8S 4M1*

(Received 15 December 2010; published 16 March 2011)

Measurements consisting of γ-ray excitation functions and angular distributions were performed using the $(n,n'\gamma)$ reaction on ^{62}Ni. The excitation function data allowed us to check the consistency of the placement of transitions in the level scheme. From γ-ray angular distributions, the lifetimes of levels up to ~3.8 MeV in excitation energy were extracted with the Doppler-shift attenuation method. The experimentally deduced values of reduced transition probabilities were compared with the predictions of the quadrupole vibrator model and with large-scale shell model calculations in the fp shell configuration space. Two-phonon states were found to exist with some notable deviation from the predictions of the quadrupole vibrator model, but no evidence for the existence of three-phonon states could be established. $Z = 28$ proton core excitations played a major role in understanding the observed structure.

DOI: 10.1103/PhysRevC.83.034316 PACS number(s): 21.10.Tg, 23.20.Lv, 25.40.Fq, 27.50.+e

I. INTRODUCTION

The stable nickel isotopes, lying above doubly magic $^{56}_{28}$Ni$_{28}$, have been the focus of many experimental and theoretical investigations over the past few decades. The closure of both the $1f_{7/2}$ proton and neutron shells in $^{56}_{28}$Ni$_{28}$ leads to a simple shell model description of the low-lying levels in nickel isotopes with proton shells completely inert and valence neutrons in the $2p_{3/2}$, $1f_{5/2}$, and $2p_{1/2}$ orbitals. Shell model calculations with this simple configuration space reproduce the energy spectra of the nickel isotopes up to ~3 MeV [1–3]; however, calculations of electromagnetic transition rates do not reproduce the experimental values. This failure indicates the necessity for excitations of the ^{56}Ni core. In fact, the excitation of both protons and neutrons from the $1f_{7/2}$ core orbital to the higher orbitals of the fp shell is required to reproduce the experimentally observed systematic trends of both g factors and B(E2)'s of the first 2^+ states of the even-even nickel isotopes with $A = 56$–68 [4,5].As seen from Fig. 1, the $B(\mathrm{E2}; 2_1^+ \rightarrow 0_1^+)$ values vary systematically with number of neutrons and *ideally* should become a maximum at ^{62}Ni, which lies at the middle of the fp shell (beyond the ^{56}Ni core). But more recent values adopted in Ref. [6] for the even-even Ni isotopes in the entire fp shell region indicate the maximum $B(\mathrm{E2}; 2_1^+ \rightarrow 0_1^+)$ for ^{60}Ni. However, this B(E2) is large in ^{62}Ni and indicates collectivity at low excitation energy. The small value of $Q(2_1^+)$ [$= +0.05(12)$ b] [7] reveals a nearly spherical shape, and the collectivity is expected to appear in terms of vibrational motion, with the onset of a sequence of quadrupole vibrational phonon states [8]. The experimental value of $E_{4^+}/E_{2^+} \sim 2$ is suggestive of considering this nucleus as a "spherical harmonic vibrator" and a 0_2^+, 2_2^+, and 4_1^+ triplet of levels does exist at approximately twice the energy of the one-phonon 2_1^+ state. Also, the energy level scheme at higher excitation exhibits close-lying levels at approximately thrice the energy of the one-phonon state. For a true categorization, one would need to identify the underlying single-particle and multiphonon contributions by obtaining B(E2) values for the associated transitions. Large E2 decay strengths (>10 W.u.) are important properties of levels to be identified as multiphonon excitations.

Numerous experiments have previously been performed in order to study the low-lying structure of ^{62}Ni. These studies include Coulomb excitation [4], β-decay measurements [9,10], transfer reactions [11–13], fusion-evaporation reactions [14], and inelastic scattering measurements with electrons [15], protons [16], neutrons [17], α particles [18], etc. According to the latest compilation in the Nuclear Data Sheets (NDS) [19], lifetimes of most of the levels in ^{62}Ni up to $E_x \sim 3.8$ MeV are known. However, as mentioned in the NDS [19], lifetimes of many of the levels previously measured with the $(n,n'\gamma)$ reaction [17] deviate from the average lifetime values obtained with other reaction studies.

With the aim of obtaining a consistent image of the properties of low-spin levels, measurements were carried out using the Doppler-shift attenuation method (DSAM) following inelastic neutron scattering from an enriched ^{62}Ni sample with neutron energies close to the threshold values of the respective

*anagha@pa.uky.edu; on leave from the Department of Physics, Krishnath College, Berhampore 742101, India.
†Present address: Department of Physics, University of the Western Cape, P/B X17, Bellville, ZA-7535 South Africa.
‡Present address: Tandem Accelerator Laboratory, Institute of Nuclear Physics, NCSR "Demokritos", 15310 Aghia Paraskevi, Athens, Greece.
§Present address: Department of Physics, University of Winnipeg, Winnipeg, MB R3E 2B9, Canada.
‖Present address: Radiation Monitoring Devices, Inc., Watertown, Massachusetts 02472, USA.

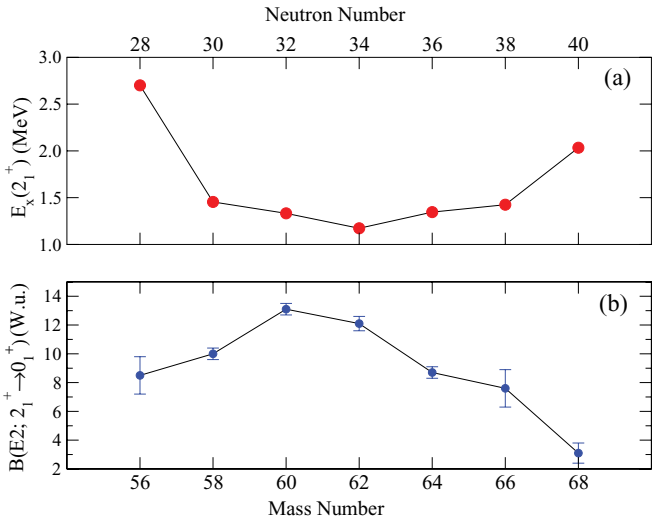

FIG. 1. (Color online) Even-even nickel isotopes within fp shell region showing the variation of excitation energies of the 2_1^+ state (top panel) and of B(E2)'s (bottom panel) as a function of mass number. The data were taken from Ref. [6]. Lines have been drawn through the data points to guide the eye.

levels. Attempts were also made to extract previously unknown spectroscopic properties, such as mixing ratios and reduced transition probabilities of many of the transitions. The search for the weak decay branches, as needed for testing the proper identification of multiphonon states, was an additional motivation behind this work.

Garrett *et al.* [20,21] recently pointed out the possibility of a breakdown of vibrational motion in the even-even stable Cd isotopes, which had long been considered as the best examples of nuclear quadrupole vibrational degrees of freedom. The ^{62}Ni isotope has also long been considered as a possible candidate for a quadrupole vibrator, and there exists an extensive literature describing the two-phonon states; however, the existence of three-phonon states is not clear. Hence, a detailed spectroscopic investigation for ^{62}Ni has been undertaken with the aim of elucidating the nature of multiphonon vibrations in this nucleus.

II. EXPERIMENTAL DETAILS AND DATA ANALYSIS

Low-lying levels of ^{62}Ni were populated with the ^{62}Ni$(n,n'\gamma)$ reaction using the 7-MV Van de Graaff accelerator facility at the University of Kentucky. The approximately monoenergetic ($\Delta E_n \sim 60$ keV) pulsed neutron fluences were produced with pulsed proton beams through the ^{3}H(p,n) reaction [22]. The $^3H_2$ gas, at a pressure of about 1 atm, was contained in a cylindrical cell approximately 3 cm long and 1 cm in diameter separated from the beam-line vacuum by a 3.5-μm-thick Mo foil. Proton beams from the accelerator were pulsed at a 1.875-MHz rate with a pulse width of $\sim$1 ns. The pulsed neutrons emerging from the gas cell were incident on a 19.39-g Ni sample, enriched to 96.46% in ^{62}Ni. The primary "contamination" in the sample arises from ^{58}Ni and ^{60}Ni, which were present with abundances of 1.87% and 1.32%, respectively. The metallic ^{62}Ni powder was tightly packed into a polypropylene container of 3.3-cm height and 2.1-cm inner diameter, which was suspended at a distance of 4.7 cm from the end of the tritium gas cell and at an angle of 0° relative to the beam direction. The γ rays produced following inelastic scattering of neutrons from the sample were detected by using a $\sim$50% (relative) efficient high-purity germanium (HPGe) detector with the resolution of $\sim$1.8 keV at 1.3 MeV. The detector was placed at a distance of $\sim$1.2 m from the sample and placed inside a bismuth germanate (BGO) anti-Compton shield to suppress unwanted Compton background [23]. Furthermore, additional shielding of tungsten, lead, copper, and boron-loaded polyethylene was used to prevent neutrons from the gas cell striking the detector. Time-of-flight gating was implemented to further suppress background radiation and to improve the quality of the spectra. The neutron flux was monitored by using a BF_3 proportional counter (which provides a nearly flat response to varying neutron energies) placed at 90° relative to the incident beam axis and at a distance of $\sim$3 m from the gas cell. The neutron flux was further monitored by observing the time-of-flight spectra of neutrons in a fast liquid scintillator (NE218). This detector was placed at a distance of 5.47 m from the gas cell and at an angle of 43° relative to the axis of the incident beam. Energy and efficiency calibrations of the HPGe detector were performed with radioactive sources, such as ^{226}Ra and ^{24}Na. Additional descriptions of the experimental setup may be found elsewhere [22,24]. Off-line spectral analysis was performed using the Tv [25] software package.

γ-ray excitation function measurement. A γ-ray excitation function measurement was carried out with the aim of clarifying the low-energy, low-spin level scheme and included measuring the yields of the γ rays produced in neutron scattering as a function of the incident neutron energy. The detector was placed at a fixed angle of 90° with respect to the axis of the incident beam. γ-ray yields were measured by varying the energy of the incident neutrons from 2.8 to 4.1 MeV in 100-keV steps. These data were used to determine the thresholds for the populated levels and usually helped the identification of γ rays decaying from particular levels, because the transitions originating from the same level should have the same threshold and similar variation of yield with neutron energy. The excitation function data were used to check the correctness of the previously known level scheme and to assign newly found decay branches.

γ-ray angular distribution measurements. For the angular distribution measurements of deexciting γ rays, incident neutron energies were chosen as close to threshold for exciting the levels as was consistent with obtaining yields with good statistics. This approach diminishes the effect of feeding from higher-lying levels that could affect both angular anisotropies and measured lifetimes. These considerations led us to undertaking angular distribution measurements at neutron energies of 2.8, 3.5, and 3.8 MeV. Spectra were recorded at 10–12 different angles, typically from 40° to 149°. An in-beam γ-ray spectrum obtained from the HPGe detector, located at 90°, with an incident neutron energy of 3.8 MeV is depicted in Fig. 2. The observation of many transitions with good statistics is obvious from the figure.

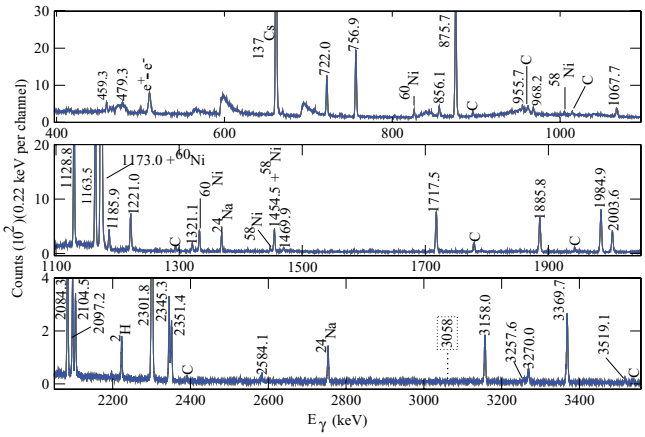

FIG. 2. (Color online) γ-ray spectrum obtained from the HPGe detector at an angle of 90° from the ^{62}Ni$(n,n'\gamma)$ reaction at an incident neutron energy of 3.8 MeV. Peaks labeled by their energies belong to ^{62}Ni. γ rays from ^{58,60}Ni, which were present as minor components in the sample, have been marked. Transitions marked as C correspond to the known laboratory background lines. Transitions from the decay of the radioactive ^{137}Cs and ^{24}Na sources, which were placed in close proximity to the HPGe detector, have also been labeled. The position of a 3058-keV γ ray is shown in the figure (see text for details).

Lifetimes of many of the excited levels were extracted from the angular distribution measurements. The lifetime of a particular level was measured by considering the Doppler shifts of the γ ray(s) decaying from the level as a function of emission angle, using the methodology described in Ref. [26]. The energy of the γ ray, $E_\gamma(\theta)$, as a function of the emission angle θ relative to the incident beam direction is governed by the relation,

$$E_\gamma(\theta) = E_0\left(1 + F(\tau)\frac{v_{\text{c.m.}}}{c}\cos\theta\right), \qquad (1)$$

where E_0 is the energy of the unshifted γ ray, $F(\tau)$ is the experimental Doppler-shift attenuation factor, $v_{\text{c.m.}}$ is the recoil velocity of the nucleus in the center-of–mass frame, and c is the velocity of light. The lifetime of the level of interest was determined by comparing the measured $F(\tau)$ values [following Eq. (1)] with those calculated using the Winterbon formalism [27]. In these angular distribution measurements, the HPGe detector was also constantly viewed by radioactive ^{24}Na and ^{137}Cs sources. The γ rays recorded from these sources along with long-lived known neutron capture γ rays from Ge were used to give a precise internal energy calibration of the data during the off-line analysis. This precise energy measurement was necessary, because angle-dependent shifts of most of the γ rays were at most a few tenths of a keV.

The angular distribution data were also used to determine the multipolarities of the deexciting γ rays. For this process, the variation of yield of a particular γ ray as a function of angle θ was fitted with a polynomial of the form

$$W(\theta) = A_0[1 + a_2P_2(\cos\theta) + a_4P_4(\cos\theta)], \qquad (2)$$

where the angular distribution coefficients a_2 and a_4 depend on the level spins, multipolarities, and mixing ratios of the transitions involved. The experimental values of the angular distribution coefficients were then compared to the results from the statistical model, obtained from a modified version of the code CINDY [28] to determine the multipolarities, with possible mixing ratio values, of the γ rays.

III. EXPERIMENTAL RESULTS

The experimental results obtained from the present experiment have been summarized in Table I. The $\overline{F(\tau)}$ for a level, as listed in Table I, is the weighted average of the $F(\tau)$ values of γ rays decaying from a particular level. The uncertainties provided for the values of $\overline{F(\tau)}$ are statistical values. Also, a systematic uncertainty of 10% due to the uncertainty of stopping powers [29] has been included in quadrature for the error estimation of the measured lifetime values. For many of the cases, two values of the mixing ratio (δ) for a particular transition are given in the table, and the rationale for acceptance of one or both values is explained in the text. The determination of the lifetime of a level by DSAM following inelastic neutron scattering works well when the level lifetime is greater than a few femtoseconds and less than about one picosecond. The lifetimes of many of the levels of interest were found to be near or above the range of optimum sensitivity of the present experimental method. Thus, the reported lifetimes for many of the levels have substantial uncertainties and, for some of the cases, only upper limits could be established.

Comparisons between level lifetimes obtained from the present experiments and the values in the ENSDF database [30] are made in Table II. Also, the table indicates lifetime values for some of the levels obtained from the earlier measurements [17], using the $(n,n'\gamma)$ reaction with reactor neutrons as a probe. Plots of variation of energies of a few transitions as a function of cos θ are depicted in Fig. 3. The lines indicate the linear fits to the experimental data, from which the $F(\tau)$ values were determined.

Details about the levels observed, up to $E_x = 3.7$ MeV in the present work, have been tabulated in Table I. The levels at 3.262, 3.378, 3.462, 3.486, and 3.500 MeV, reported in the NDS [19], were not observed in the present experiment. Also, a few transitions observed in the excitation function data could not be placed in the level scheme. These include γ rays [observed at minimum neutron energies (MeV)] at 415 [3.6], 1421 [3.9], and 2689 [4.0] keV.

Experimental spectroscopic features associated with some of the observed states up to 3.7 MeV excitation are highlighted below. This discussion is limited to those states for which either new findings have been established in the present investigation or there is special interest related to the phonon vibrations. Lifetime values for all the states are presented in terms of mean lives.

A. 2_1^+ state at 1173.0 keV

The lifetime of the first excited state has been reported in a number of earlier studies; the most recent work is by Kenn *et al.* [4]. Combining the results from Refs. [4,31], the accepted lifetime of the level is found to be $\tau = 2.09(6)$ ps [30]. As our method is not very sensitive to lifetimes in this range, a large uncertainty is associated with our value (see Table II), hence we defer to the value reported in Ref. [30]. Using this

TABLE I. Excitation energies of levels (E_x), γ-ray energies (E_γ), initial (J_i^π) and final (J_f^π) spins, relative γ-ray intensities (I_γ), average attenuation factors [$\bar{F}(\tau)$], mean lifetimes (τ), mixing ratios (δ) or multipolarities (πL), and reduced transition probabilities for transitions in ^{62}Ni. Newly assigned quantities from the present investigation are highlighted in italics.

E_x (keV)	E_γ (keV)	$J_i^\pi \to J_f^\pi$	I_γ (%)	$\bar{F}(\tau)$	τ (ps)	δ or πL	B(M1)↓ (μ_N^2)	B(E2)↓ (W.u.)
1173.0(1)	1172.95(11)	$2_1^+ \to 0_1^+$	100	0.021(7)	$1.79^{+0.86}_{-0.48}$	E2		$14.1^{+5.1}_{-4.6}$
2048.7(1)	875.69(7)	$0_2^+ \to 2_1^+$	100	0.013(7)	$2.6^{+2.7}_{-0.9}$	E2		42^{+23}_{-21}
2301.8(1)	1128.82(14)	$2_2^+ \to 2_1^+$	44.7(11)	0.034(7)	$0.96^{+0.29}_{-0.20}$	$2.70^{+0.38}_{-0.28}$	0.002(1)	$12.5^{+3.8}_{-3.2}$
	2301.83(30)	$2_2^+ \to 0_1^+$	55.3(18)			E2		$0.50^{+0.13}_{-0.12}$
2336.5(1)	1163.50(12)	$4_1^+ \to 2_1^+$	100	0.027(8)	$1.23^{+0.59}_{-0.32}$	E2		$21.4^{+7.6}_{-7.0}$
2890.5(3)	1717.53(33)	$0_3^+ \to 2_1^+$	100		>4.5[a]	E2		<0.84
3058.8(2)	722.02(23)	$3_1^+ \to 4_1^+$	19.8(15)		$3.3^{+2.0}_{-1.0}$[a]	$1.60^{+0.29}_{-0.90}$	$0.003^{+0.006}_{-0.002}$	$12.3^{+6.9}_{-8.8}$
	756.85(20)	$3_1^+ \to 2_2^+$	41.9(26)			$-0.08(2)$	$0.016^{+0.008}_{-0.006}$	$0.18^{+0.23}_{-0.12}$
	1885.84(34)	$3_1^+ \to 2_1^+$	38.3(32)			$-0.03^{+0.03}_{-0.02}$	0.0010(4)	$0.0002^{+0.0008}_{-0.0002}$
3157.9(2)	856.09(12)	$2_3^+ \to 2_2^+$	7.2(3)	0.041(5)	$0.89^{+0.16}_{-0.14}$	$1.92^{+0.39}_{-0.29}$	$0.0016^{+0.0008}_{-0.0006}$	$7.8^{+2.1}_{-1.7}$
						0.09(7)	$0.007^{+0.002}_{-0.001}$	$0.08^{+0.21}_{-0.08}$
	1984.93(28)	$2_3^+ \to 2_1^+$	58.6(25)			−0.13(3)	$0.0047^{+0.0010}_{-0.0007}$	$0.02^{+0.02}_{-0.01}$
						$3.77^{+0.70}_{-0.52}$	$0.0003^{+0.0002}_{-0.0001}$	$1.12^{+0.24}_{-0.19}$
	3158.04(151)	$2_3^+ \to 0_1^+$	34.2(38)			E2		0.07(1)
3176.8(3)[b]	875.0(4)	$4_2^+ \to 2_2^+$	6.5(10)	0.008(17)	>1.4	E2[c]		<5.0
	2003.63(42)	$4_2^+ \to 2_1^+$	93.5(39)			E2		<1.1
3257.5(2)	*955.65(28)*	$2_4^+ \to 2_2^+$	3.5(2)	0.013(11)	>1.4	E2 + M1[c]		
	2084.25(41)	$2_4^+ \to 2_1^+$	93.4(28)			$1.03^{+0.22}_{-0.70}$	<0.004	<0.6
						$0.43^{+0.90}_{-0.12}$	<0.004	<0.6
	3257.57(120)	$2_4^+ \to 0_1^+$	3.1(4)			E2		<0.003
3270.0(2)[d]	968.20(45)	$(1_1^+,2_5^+) \to 2_2^+$	>5	0.172(7)	*0.18(2)*	E2 + M1[c]		
	1221.04(26)	$(1_1^+,2_5^+) \to 0_2^+$	<42			M1, E2[c]		
	2097.15(26)	$(1_1^+,2_5^+) \to 2_1^+$	>43			E2 + M1[c]		
	3270.00(223)	$(1_1^+,2_5^+) \to 0_1^+$	>10			M1, E2[c]		
3277.7(3)	2104.52(32)	$4_3^+ \to 2_1^+$	100	0.058(7)	$0.60^{+0.10}_{-0.09}$	E2		$2.3^{+0.4}_{-0.3}$
3369.6(2)	479.25(64)	$I_{1,2}^+ \to 0_3^+$	2.1(4)	0.068(12)	$0.51^{+0.12}_{-0.09}$	M1[c]	$0.021^{+0.005}_{-0.004}$	
	1067.71(26)	$I_{1,2}^+ \to 2_2^+$	12.6(13)			$1.6^{+4.1}_{-1.1}$	$0.003^{+0.008}_{-0.003}$	$7.2^{+4.6}_{-5.6}$
	1321.11(33)	$I_{1,2}^+ \to 0_2^+$	9.7(10)			M1[c]	0.005(1)	
	3369.68(168)	$I_{1,2}^+ \to 0_1^+$	75.6(124)			M1	$0.0022^{+0.0005}_{-0.0004}$	
3518.3(2)	*360.49(40)*	$2_{5,6}^+ \to 2_3^+$	1.9(2)	0.039(5)	$0.90^{+0.18}_{-0.15}$	E2 + M1[c]		
	459.30(28)	$2_{5,6}^+ \to 3_1^+$	7.4(4)			E2 + M1[c]		
	1469.88(50)	$2_{5,6}^+ \to 0_2^+$	9.8(4)			E2		$0.89^{+0.18}_{-0.15}$
	2345.33(42)	$2_{5,6}^+ \to 2_1^+$	73.7(36)			0.32(6)	$0.0033^{+0.0008}_{-0.0007}$	$0.06^{+0.04}_{-0.03}$
						1.20(13)	$0.0015^{+0.0005}_{-0.0004}$	$0.38^{+0.12}_{-0.09}$
	3519.08(213)	$2_{5,6}^+ \to 0_1^+$	7.3(11)			E2		$0.008^{+0.002}_{-0.001}$
3522.5(2)[f]	264.94(25)[e]	$(3_2^+) \to 2_4^+$		0.040(13)	$0.88^{+0.43}_{-0.24}$	E2 +M1[c]		
	463.33(48)	$(3_2^+) \to 3_1^+$	>4			E2 +M1[c]		
	1185.94(18)	$(3_2^+) \to 4_1^+$	>24			$-20.5^{+7.8}_{-43.1}$	$0.00003^{+0.00007}_{-0.00003}$	$8.3^{+3.1}_{-2.7}$
	1221.04(26)	$(3_2^+) \to 2_2^+$	<72			E2 +M1[c]		
3524.6(3)	*2351.41(43)*	$0_4^+ \to 2_1^+$	100	0.033(12)	$1.07^{+0.66}_{-0.32}$	E2		$0.73^{+0.31}_{-0.28}$
3756.4(3)	1454.53(32)[g]	$3_1^- \to 2_2^+$	48(4)	0.128(37)	$0.24^{+0.12}_{-0.07}$	E1[c]		
	2584.11(52)[h]	$3_1^- \to 2_1^+$	52(4)			E1		

[a]Adopted from the data base of Ref. [30].

[b]Probably there is a γ ray with a transition energy of 840 keV from the state, but it has not been placed due to the lack of sufficient statistics (see text for details).

[c]Experimental angular distribution coefficients could not be measured. The assumed multipolarity is based upon the spins of the initial and final states involved.

[d]Due to the presence of a doublet, the intensity of the 1221.04-keV transition could not be measured accurately. Hence, only the limits of the decay branches have been reported. With the feeding from the doublet transition, the measured intensities of the decay branches [968.20, 1221.04, 2097.15, and 3270.00 keV] are found to be 4.8(2):38.9(10):44.7(13):11.6(14).

[e]Due to poor statistics, the intensity of the 264.94-keV transition could not be measured from the present experiment.

[f]Due to the presence of a doublet, the intensity of the 1221.04-keV transition could not be directly measured. Without considering the weakest 264.94-keV decay branch and considering the feeding from the doublet transition, the measured intensities of the decay branches [463.33, 1185.94, and 1221.04 keV] are found to be 4.6(3):24.8(6):70.7(16).

[g]A value of $B(E1)\downarrow = 4(2) \times 10^{-4}$ W.u. was obtained for this transition from the present lifetime value.

[h]A value of $B(E1)\downarrow = 8^{+2}_{-3} \times 10^{-5}$ W.u. was obtained for this transition from the present lifetime value.

TABLE II. Comparison of level lifetimes of ^{62}Ni extracted from the present measurement (τ_{pres}) with those as mentioned in database (τ_{lit}) [30]. Lifetime values (τ_{prev}) [17] of a few levels from a previous $(n,n'\gamma)$ measurement have also been listed.

E_x (keV)	J^π	τ_{prev} (ps)	τ_{lit} (ps)	τ_{pres} (ps)
1173.0	2_1^+		2.09(6)	$1.79^{+0.86}_{-0.48}$
2048.7	0_2^+		$1.1^{+1.1}_{-0.4}$	$2.6^{+2.7}_{-0.9}$
2301.8	2_2^+	$0.5^{+0.8}_{-0.2}$	$0.84^{+0.23}_{-0.13}$	$0.96^{+0.29}_{-0.20}$
2336.5	4_1^+	$0.4^{+1.6}_{-0.2}$	$1.24^{+0.35}_{-0.19}$	$1.23^{+0.59}_{-0.32}$
2890.5	0_3^+		> 4.5	
3058.8	3_1^+		$3.3^{+2.0}_{-1.0}$	
3157.9	2_3^+	$0.12^{+0.03}_{-0.02}$	$0.99^{+0.79}_{-0.40}$	$0.89^{+0.16}_{-0.14}$
3176.8	4_2^+		1.05(25)	>1.4
3257.5	2_4^+		1.03(25)	>1.4
3270.0	$(1_1^+,2_5^+)$			0.18(2)
3277.7	4_3^+	$0.6^{+1.9}_{-0.7}$	$0.28^{+0.05}_{-0.03}$	$0.60^{+0.10}_{-0.09}$
3369.6	$1_{1,2}^+$		0.27(13)	$0.51^{+0.12}_{-0.09}$
3518.3	$2_{5,6}^+$	$0.14^{+0.03}_{-0.02}$	0.29(6)	$0.90^{+0.18}_{-0.15}$
3522.5	(3_2^+)		$0.22^{+0.09}_{-0.07}$	$0.88^{+0.43}_{-0.24}$
3524.6	0_4^+			$1.07^{+0.66}_{-0.32}$
3756.4	3_1^-	$0.65^{+0.65}_{-0.25}$	$0.22^{+0.05}_{-0.03}$	$0.24^{+0.12}_{-0.07}$

lifetime value [30], we adopt a value of $B(E2) = 12.1(4)$ W.u. (see Table III) for the 1172.95($2_1^+ \rightarrow 0_1^+$)-keV E2 transition. This state has long been considered to be a one-phonon vibrational excitation [32].

B. 0_2^+ state at 2048.7 keV

This level decays by an 875.69-keV E2($0_2^+ \rightarrow 2_1^+$) transition. Also, Passoja *et al.* [33] observed an $E0(0_2^+ \rightarrow 0_1^+)$ decay from this state and measured the $E0$ decay rate through internal pair spectroscopy. While the lifetimes obtained in the present work ($2.6^{+2.7}_{-0.9}$ ps) and those quoted in Ref. [30] ($1.1^{+1.1}_{-0.4}$ ps) are in agreement within the experimental uncertainties, they exhibit large uncertainties. The $B(E2)$ values for the 875.69-keV transition from the present measurement and from Ref. [30] are 42^{+23}_{-21} and 100^{+58}_{-50} W.u., respectively. As the upper limit of $B(E2)$ from Ref. [30] is unreasonably large, the present value is adopted for further discussion. The observed enhancement of the $B(E2; 0_2^+ \rightarrow 2_1^+)$ value for the 875.69-keV transition supports the assignment of this state as a two-phonon vibrational excitation.

C. 2_2^+ state at 2301.8 keV

As reported in Ref. [32], this level decays with two branches. The intensities of the 1128.82- and 2301.83-keV transitions, which depopulate the 2301.8-keV state, were measured in the present experiment to be in agreement with those given in Ref. [32]. Also, the level lifetime ($\tau = 0.96^{+0.29}_{-0.20}$ ps) and mixing ratio ($\delta = 2.70^{+0.38}_{-0.28}$) for the 1128.82-keV transition extracted from the present measurement are in good agreement with the adopted value [30]. Values of $a_2 = 0.44(4)$ and $a_4 = -0.25(5)$ obtained from the present measurement also confirm the $\Delta J = 2$ E2 nature of the 2301.83-keV transition. This level has long been considered to be a candidate for a member of the two-phonon quadrupole vibrational triplet, with the characteristic enhancement of the $B(E2; 2_2^+ \rightarrow 2_1^+)$ and the associated reduction of the $B(E2; 2_2^+ \rightarrow 0_1^+)$ values.

D. 4_1^+ state at 2336.5 keV

The characteristic features of this level suggest it as a candidate for a two-phonon vibrational state. This state decays to the 2_1^+ state through a 1163.50-keV transition, and a $B(E2)$ value of $21.4^{+7.6}_{-7.0}$ W.u. was measured for this transition. As can be seen from Table II, the lifetime of this state obtained from the present experiments deviates from the earlier measurement with the $(n,n'\gamma)$ reaction [17] but is in close agreement with the value adopted in Ref. [30].

E. 3_1^+ state at 3058.8 keV

Fanger *et al.* [34], using the ^{61}Ni(n,γ) reaction, established four decay branches from this level with transitions of 722, 756, 1886, and 3060 keV having branch percentages of 15 : 35 : 39 : 11. In subsequent work by Kennedy *et al.* [32], excited states of ^{62}Ni were populated by means of the ^{59}Co$(\alpha,p\gamma)$ reaction. In that work, the 3060 keV transition was not observed. Also, using the same reaction, the spectroscopic study by Ohnuma *et al.* [35] excluded the 3060-keV crossover transition. From the apparent lack of a crossover transition, an ambiguous $l = 2$ assignment in the (p,t) angular distribution data for this state [36], and the shell model prediction by Glaudemans *et al.* [3] for a 3^+ state at about 2.8 MeV excitation, Ohnuma *et al.* [35] tentatively assigned the spin of this state as 3^+.

The 3058.8-keV level was populated strongly with the $(n,n'\gamma)$ reaction. As the present detection system seems sensitive to decay branches with strengths $>2\%$ [37], a crossover decay branch to the ground state from the 3058.8-keV level with an intensity of more than 2% would have been clearly observed. No such crossover transition was seen in either our excitation function or angular distribution data (see Fig. 2). The present experimental data reveal that the 3058.8-keV level decays via 722.02-, 756.85-, and 1885.84-keV transitions. The goodness of fit plots in Fig. 4 for the 1885.84-keV transition do not discriminate between the 3^+ and 2^+ assignments for the 3058.8-keV level. The χ^2 vs δ (E2/M1 mixing ratio) plot shows similar minima for both the assignments, but with a preference for 3^+. A similar analysis for the 756.85- and 722.02-keV transitions permits only the 3^+ assignment for their initial decay state. Also, we have observed nearly zero values of a_4 and negative values of a_2 for the three observed decay branches from this state. These features correspond to a $\Delta J = 1$ nature. This condition could be satisfied by these three transitions only if they decay from a state with spin 3^+; hence, we suggest a 3^+ spin assignment for the 3058.8-keV state. This assignment then would explain the nonobservation of a 3058-keV transition in the present experiment, as this would be a transition of M3 multipolarity. With the present

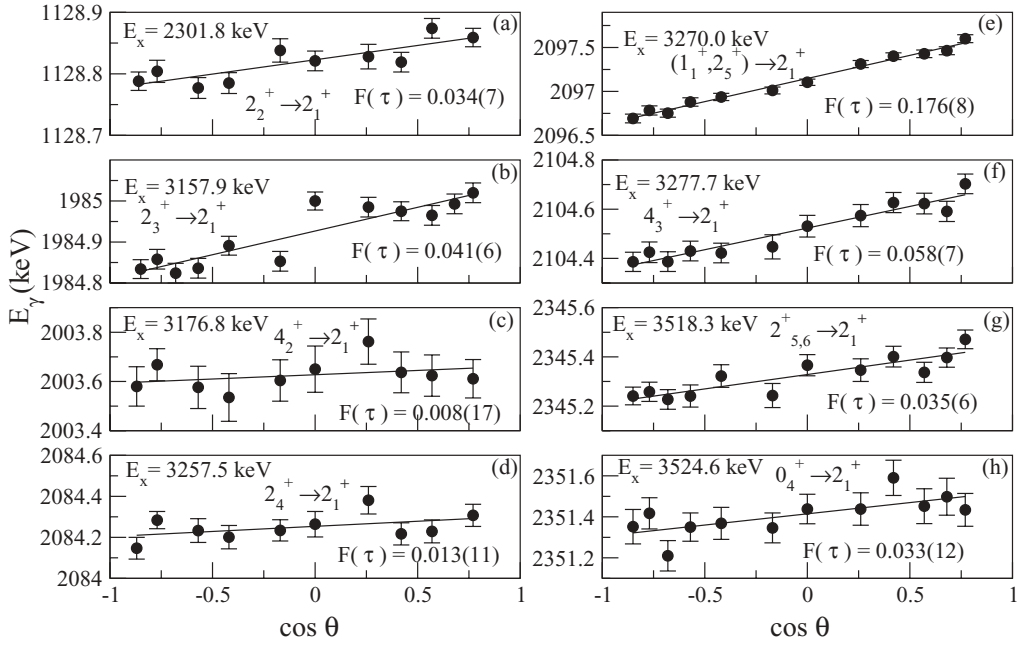

FIG. 3. Measured γ-ray energies as a function of cos θ for transitions from several levels of interest. The lines are linear fits to the data. Corresponding $F(\tau)$ values are indicated.

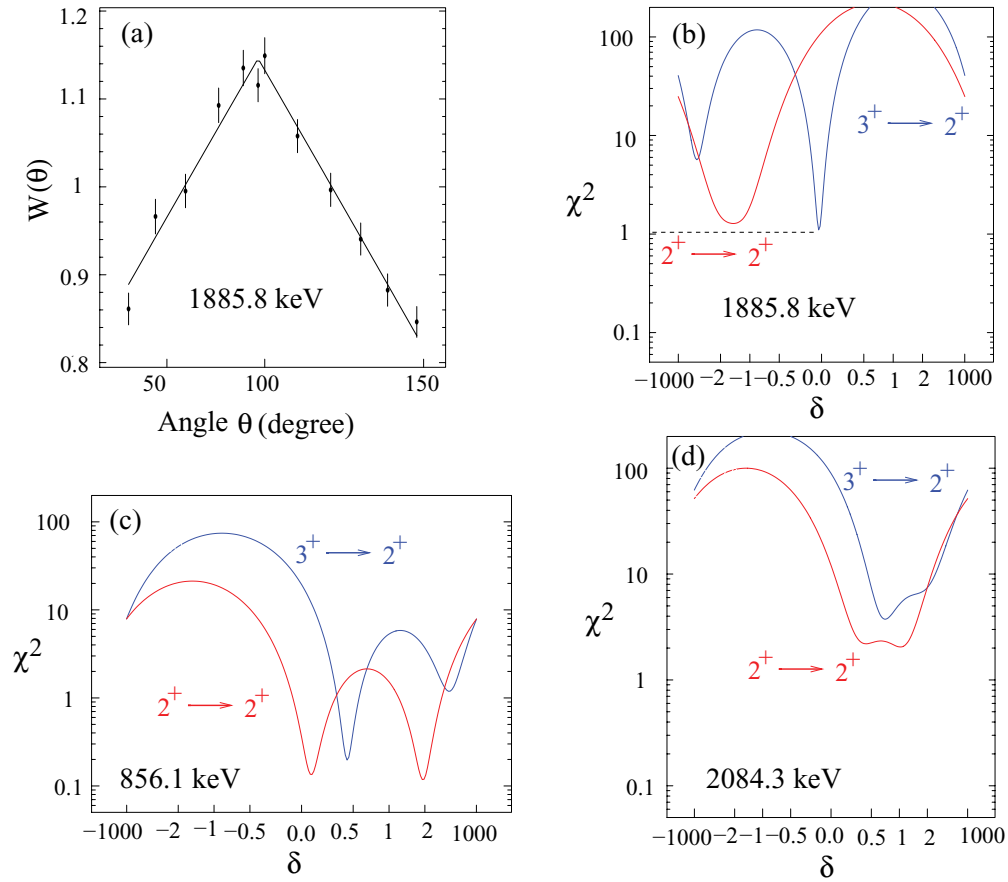

FIG. 4. (Color online) (a) Angular distribution of the 1885.8-keV γ ray from the 3058.8-keV level. A least-squares fit to these data with a polynomial of the form given in Eq. (2) leads to the angular distribution coefficients $a_2 = -0.29(2)$ and $a_4 = -0.00(3)$. The abscissa scale is linear in $\cos^2\theta$, but the axis labels indicate θ. (b) χ^2 vs δ for the 1885.8-keV γ ray. The figure indicates that $3^+ \rightarrow 2^+$ for the 1885.8-keV transition is more probable (see text for details). The horizontal dotted line is drawn just to guide the eye. (c) χ^2 vs δ for the 856.1-keV transition from the 3157.9-keV level. (d) χ^2 vs δ for the 2084.3-keV transition deexciting the 3257.5-keV level.

TABLE III. Comparison of experimental and theoretical reduced transition probabilities for ^{62}Ni. $B(\mathrm{E2})_{\mathrm{expt}}$ are experimental $B(\mathrm{E2})$ values; $B(\mathrm{E2})_{\mathrm{vib}}$ are values obtained following the harmonic quadrupole vibrator model; $B(\mathrm{E2})_{\mathrm{SM}}$ are values obtained following the shell model. Same nomenclature holds for $B(\mathrm{M1})$ as well. $B(\mathrm{E2}; 2_1^+ \rightarrow 0_1^+)_{\mathrm{vib}}$ has been normalized to the corresponding experimental $B(\mathrm{E2})$ value to facilitate the comparison. The spins of the initial (J_i^π) and the final (J_f^π) states associated with a decay transition are cited in the left most column. The $B(\mathrm{E2})_{\mathrm{expt}}$ and $B(\mathrm{M1})_{\mathrm{expt}}$ values for all the transitions reported in the table are from the present experimental work, except that for the $2_1^+ \rightarrow 0_1^+$ transition, which has been adopted from Ref. [30]. Brackets in the $B(\mathrm{E2})_{\mathrm{expt}}$ and $B(\mathrm{M1})_{\mathrm{expt}}$ columns denote the value of transition strength as obtained using the alternate possible value of the mixing ratio (see Table I) for the said transition.

$J_i^\pi \rightarrow J_f^\pi$	$B(\mathrm{E2})_{\mathrm{expt}}$ (W.u.)	$B(\mathrm{E2})_{\mathrm{vib}}$ (W.u.)	$B(\mathrm{E2})_{\mathrm{SM}}$ (W.u.)	$B(\mathrm{M1})_{\mathrm{expt}}$ (μ_N^2)	$B(\mathrm{M1})_{\mathrm{SM}}$ (μ_N^2)
$2_1^+ \rightarrow 0_1^+$	12.1(4)	12	15.5		
$0_2^+ \rightarrow 2_1^+$	42^{+23}_{-21}	24	14.4		
$2_2^+ \rightarrow 2_1^+$	$12.5^{+3.8}_{-3.2}$	24	10.4	0.002(1)	0.002
$2_2^+ \rightarrow 0_1^+$	$0.50^{+0.13}_{-0.12}$	0	0.01		
$4_1^+ \rightarrow 2_1^+$	$21.4^{+7.6}_{-7.0}$	24	18.0		
$0_3^+ \rightarrow 2_1^+$	<0.84	0	0.39		
$3_1^+ \rightarrow 4_1^+$	$12.3^{+6.9}_{-8.8}$	10.3	4.0	$0.003^{+0.006}_{-0.002}$	0.0001
$3_1^+ \rightarrow 2_2^+$	$0.18^{+0.23}_{-0.12}$	25.7	0.02	$0.016^{+0.008}_{-0.006}$	0.004
$3_1^+ \rightarrow 2_1^+$	$0.0002^{+0.0008}_{-0.0002}$	0	0.0011	0.0010(4)	0.001
$2_3^+ \rightarrow 2_2^+$	$0.08^{+0.21}_{-0.08}$	6.9	0.43	$0.007^{+0.002}_{-0.001}$	0.0027
	$[7.8^{+2.1}_{-1.7}]$			$[0.0016^{+0.0008}_{-0.0006}]$	
$2_3^+ \rightarrow 2_1^+$	$0.02^{+0.02}_{-0.01}$	0	0.46	$0.0047^{+0.0010}_{-0.0007}$	0.0004
$2_3^+ \rightarrow 0_1^+$	0.07(1)	0	0.06		
$4_2^+ \rightarrow 2_2^+$	<5.0	18.9	4.7		
$4_2^+ \rightarrow 2_1^+$	<1.1	0	0.78		
$2_4^+ \rightarrow 2_1^+$	<0.6		0.11	<0.004	0.026
$2_4^+ \rightarrow 0_1^+$	<0.003		0.09		
$4_3^+ \rightarrow 2_1^+$	$2.3^{+0.4}_{-0.3}$		4.8		
$0_4^+ \rightarrow 2_1^+$	$0.73^{+0.31}_{-0.28}$		0.06		

spin assignment, we obtain nearly zero values of δ for both the 756.85- and 1885.84-keV transitions, indicating they decay predominantly with M1 multipolarity. Observation of a nonzero δ value for the 722.02-keV transition establishes the positive parity for the 3058.8-keV state. Thus the assignment of 3^+ to this state is now definitely confirmed. With $B(\mathrm{E2}) \leqslant 0.2$ W.u. for the $3_1^+ \rightarrow 2_2^+$ 756.85-keV transition and the other data in Tables I and III, this state is not considered an appropriate candidate for a three-phonon excitation.

F. 2_3^+ state at 3157.9 keV

A more precise lifetime of this state has been obtained from the present measurement. The lifetime obtained from the present measurement is $0.89^{+0.16}_{-0.14}$ ps ; whereas the reported value in Ref. [30] is $0.99^{+0.79}_{-0.40}$ ps. The present lifetime value deviates from the value obtained in the previous $(n,n'\gamma)$ work by Kosyak *et al.* [17] (see Table II). All the transitions reported in the NDS [19] were observed in this work. For the 856.09-keV transition, two δ solutions were obtained, with more or less equal χ^2 values [see Fig. 4(c)]. Hence the preference for one δ value over the other could not be ascertained from the present experimental data. However, better agreement of the experimental and theoretical $B(\mathrm{E2}; 2_3^+ \rightarrow 2_2^+)$ values was obtained (see Table III) with a value of $\delta = 0.09(7)$. Similarly, out of two possible values, the δ adopted for the 1984.93-keV transition is $-0.13(3)$, which is in close agreement with the accepted value [19]. The ground-state crossover 3158.04-keV transition was found to possess a positive $a_2 = 0.38(3)$ and a negative $a_4 = -0.04(4)$, which confirms E2 multipolarity. With a measured $B(\mathrm{E2})$ of $0.08^{+0.21}_{-0.08}$ W.u. for the $2_3^+ \rightarrow 2_2^+$ transition, this state does not appear to be a three-phonon vibrational excitation.

G. 4_2^+ state at 3176.8 keV and 2_4^+ state at 3257.5 keV

In accordance with the NDS [19], all the decay branches from these two states have been observed. In addition, a new 955.65-keV transition from the 3257.5 keV state has been observed. Lifetime values of both the states were found to be somewhat larger than what had been accepted in the latest compilation [30] (see Table II). From the present measurements, only lower limits of 1.4 ps were obtained for both these states; whereas the reported lifetimes [30] are about 1 ps. Two possible values of mixing ratios were obtained for the 2084.25 ($2_4^+ \rightarrow 2_1^+$)-keV transition [see Table I and Fig. 4(d)]. Both values provide similar χ^2 values and hence both are equally likely. As can be seen from Table I, both values of the mixing ratio with the associated uncertainty give a similar upper limit of $B(\mathrm{E2})$ and $B(\mathrm{M1})$ for this transition. There is an indication of a 840- keV peak in the excitation function spectra, which might be a possible $4_2^+ \rightarrow 4_1^+$ decay transition. But the weak peak lies

on a recoil broadened background, and sufficient spectroscopic information could not be extracted. Thus, we have not been able to place the transition in the present level scheme. From the energy of the 4_2^+ state, one might expect it to be a possible member of a three-phonon quintuplet, but the available information is insufficient to associate this state with a phonon structure.

H. $(1_1^+, 2_5^+)$ state at 3270.0 keV

Possible spin values of 1^+ and 2^+ are tentatively suggested for this state in the NDS [19]. There is no reported lifetime for this state in the current data base [30]. From the present measurement, a lifetime of $\tau = 0.18(2)$ ps has been obtained. Though the present shell model calculation indicates a preference for a 1^+ state at this excitation energy, the experimental angular anisotropies could not be obtained for the decay branches. Hence, the spin assignment for this state remains ambiguous.

I. 4_3^+ state at 3277.7 keV

An assignment of 4^+ for this state was earlier made by Kong-A-Siou and Nann [36] through the study of the ^{64}Ni$(p,t)^{62}$Ni reaction. The present angular distribution measurement of the 2104.52-keV transition confirms this assignment, as the angular distribution coefficients of $a_2 = 0.42(2)$ and $a_4 = -0.14(3)$ reveal $\Delta J = 2$. However, as can be seen from Table II, the lifetime obtained from the present investigation is found to be somewhat longer than the accepted value [30].

J. $1_{1,2}^+$ state at 3369.6 keV

Possible spin values of 1^+ or 2^+ are suggested for this state in the NDS [19]. The intensity value reported for the 1321.11-keV transition might be ambiguous due to its plausible contamination from a γ ray belonging to ^{58}Ni in the same energy region. The 3369.68-keV ground state transition has been observed with good statistics in the present experiment. Values of $a_2 = -0.26(3)$ and $a_4 = 0.01(3)$, obtained from the angular distribution measurement, are suggestive of the stretched dipole character of the transition and helps us to assign unambiguously a spin value of 1 for the state. Also, the nonzero δ value for the 1067.71-keV transition to the 2_2^+ state is suggestive of no change of parity between the initial and final states associated with this transition. Hence, an unambiguous spin-parity assignment of 1^+ has been made for the state.

K. $2_{5,6}^+$ state at 3518.3 keV

In addition to all the transitions reported in the NDS [19], a newly found 360.49-keV γ ray from this state has been placed. Two possible δ values, 0.32(6) and 1.20(13), have been obtained for the $2345.33(2^+ \rightarrow 2^+)$-keV transition at two different χ^2 values. With preference for the minimum χ^2, $\delta = 0.32(6)$ has been accepted as the more likely. This value is in close agreement with that reported in the NDS [19].

L. (3_2^+) state at 3522.5 keV

This state has been assigned with possible spin values of 2^+ and 3^+ in the NDS [19]. The 264.94-keV transition was observed, but we were unable to find its intensity due to weak statistics. Also, the intensity of the 1221.04-keV transition could not be measured because of the presence of another 1221-keV transition from the 3270.0-keV state. Hence, only the limits for the relative intensities of the decay branches could be obtained (see Table I). The angular distribution measurement of the contamination-free and stronger decay branch, the 1185.94-keV transition, yielded $a_2 = -0.22(5)$ and $a_4 = 0.06(7)$. These correspond to the values expected for a $\Delta J = 1$ transition. Although the minimum χ^2 for δ was obtained with a $3^+ \rightarrow 4^+$ assignment, the present statistics yield large uncertainty. Hence, the state has been tentatively assigned a spin of 3^+.

M. 0_4^+ state at 3524.6 keV

This newly established level, with a lifetime of $1.07^{+0.66}_{-0.32}$ ps, is placed by the observation of a 2351.41-keV transition which decays to the 2_1^+ state at 1173.0 keV. As shown in Fig. 2, two close-lying peaks with transition energies of 2345.33 and 2351.41 keV are well resolved in the spectrum recorded by the HPGe detector at 90° with an incident neutron energy of 3.8 MeV. From the measured peak area, we found that the 2351.41-keV transition is 0.7 times stronger than the previously well-known 2345.33-keV transition. Also, we observed nearly the same threshold for both transitions in the excitation function data. From the angular distribution data, it was observed that the 2351.41-keV transition is isotropic with a measured $a_2 = -0.03(7)$ and can be assigned with 0^+ for its initial decay state [38]. Anisotropy of a γ ray might not be measured from the angular distribution when a state has a long lifetime or if it is fed heavily from higher-lying transitions. Since, in the present experiment, the 2351.41-keV transition exhibits good statistics with the neutron energy close to its threshold, the observed isotropy of the angular distribution data reveals its $0^+ \rightarrow 2^+$ decay nature. The observation of this 0^+ state is corroborated by the work of Stein *et al.* [12], who used the $(^6$Li,$d)$ reaction to populate the excited states of ^{62}Ni. A strongly populated 0^+ state at 3519-keV excitation, with probable uncertainty of about 10 keV, was observed in their work. It is worthwhile to point out that from the energy difference between the (3_2^+) and 2_1^+ states, the observed threshold and $F(\tau)$ value, the 2351.41-keV transition is a possible decay branch from the (3_2^+) state. But the observed isotropy in the angular distribution suggests that this transition decays from the new 0_4^+ state.

IV. THEORETICAL CALCULATIONS AND DISCUSSION

The experimental data obtained from the present investigation have been interpreted both on the basis of a "quadrupole vibrator" model and through shell model calculations.

As can be seen in Fig. 5, the three close-lying levels at $\sim$2 MeV appear to be good candidates for two-phonon states, with the vibrational 0_2^+, 2_2^+, and 4_1^+ triplet of states at about

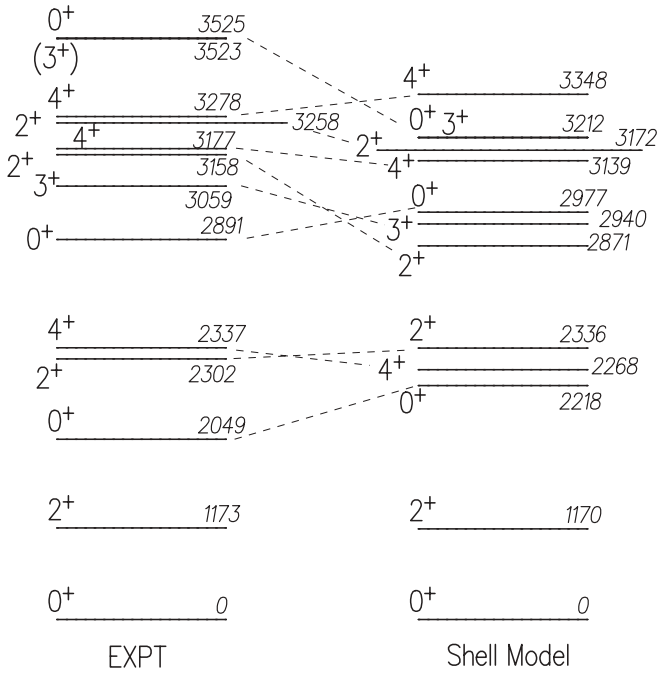

FIG. 5. Comparison of experimental and theoretical (shell model) level energies. Levels have been labeled by their corresponding excitation energies in keV, but the scale is not linear.

twice the energy of the one-phonon first 2^+ state. Also, from the point of view of their energies, the close-lying 0_3^+, 2_3^+, 4_2^+ states and the newly assigned 3_1^+ state at about 3 MeV excitation are possible candidates for three-phonon states. The known $(6)^+$ state [19], which might be considered as a possible member for the quintuplet of three-phonon states, lies several hundred keV above the rest of the candidates for members of the quintuplet; no further discussion of this state will be presented.

Let us first limit the discussion to how well the measured quadrupole properties, primarily of the two- and three-phonon states, agree with the predictions of the simple quadrupole-vibrator model. As can be seen from Table III, the generally accepted two-phonon vibrational states show deviations from the vibrational predictions. With a large uncertainty, but a significantly revised experimental E2-transition strength, the two- to one-phonon $0_2^+ \rightarrow 2_1^+$ transition appears to be in agreement (within the range of the lower limit) with the expected vibrator strength. On the other hand, the experimental $B(\mathrm{E2})$ for the $2_2^+ \rightarrow 2_1^+$ transition is smaller by a factor of 2 than the prediction of the vibrator model. The hindrance observed for the $2_2^+ \rightarrow 0_1^+$ transition is in accordance with the vibrational model, as this would involve the destruction of two phonons. Also, the experimentally observed transition strength for $4_1^+ \rightarrow 2_1^+$ matches well with the expected vibrator strength. Thus, it might be summarized that the two-phonon vibrational structure seems to persist in ^{62}Ni.

The scenario for three-phonon states could not be supported because of the absence of transitions decaying from the presumed three-phonon states to two-phonon states. These include $0_3^+ \rightarrow 2_2^+$, $2_3^+ \rightarrow 0_2^+$, and $2_3^+ \rightarrow 4_1^+$. According to the vibrator model, these missing transitions should carry a significant amount of E2 strength. Interestingly, the expected branchings from the shell model calculations are about 1% for these transitions and beyond the detection limit of the present experiments. The shell model calculation also predicts a branching of ∼6% for the $4_2^+ \rightarrow 4_1^+$ transition. In fact, we have observed a transition with an energy of ∼840 keV corresponding to the difference of energy between the experimental 4_2^+ and 4_1^+ states. But, as mentioned above, the transition could not be placed in the level scheme due to the lack of sufficient statistics. Although the experimental E2 decay strength for the $3_1^+ \rightarrow 4_1^+$ transition is in agreement with the vibrator model, hindrance by two orders of magnitude has been obtained for the $3_1^+ \rightarrow 2_2^+$ transition from the expected vibrator strength. A similar type of deviation also persists in the decay behavior of the 4_2^+ state. The observed E2 decay behavior of the 2_3^+ state is in accordance with the vibrator model, but the nonobservation of other expected decay branches has made it difficult for a firm assignment of three-phonon character even to this state. Thus three-phonon excitations appear to be inconsistent with the present data.

For a microscopic description of the low-lying states in ^{62}Ni, a theoretical calculation has been carried out in the frame work of the spherical shell model. Proper choice of model space and effective interaction is the key ingredient for the success of this type of calculation. From a simplistic point of view, the closure of the $1f_{7/2}$ proton and neutron orbitals in the doubly magic nucleus $^{56}_{28}\mathrm{Ni}_{28}$ might lead to a good shell model description of the low-lying excited states in $^{62}_{28}\mathrm{Ni}_{34}$ with the proton orbitals completely inert and treating the six valence neutrons distributed in the $2p_{3/2}$, $1f_{5/2}$, and $2p_{1/2}$ orbitals. Shell model calculations with this restricted model space could reproduce the experimental level spectra quite successfully up to ∼3 MeV excitation energy, but for a reasonable description of electromagnetic transition rates, unrealistically large values of effective charges were required [33]. This suggests too much restriction of the model space used and that the excitations of the ^{56}Ni core are important for the proper description of the observed level structure. The more recent experimentally measured positive value of the g factor [4] for the 2_1^+ state in ^{62}Ni also points toward the importance of the proton contributions in the wave function of the underlying states. Hence, proton excitations across the $Z = 28$ shell closure seem to be essential. It has been shown that as many as ten nucleons could be excited across the $Z = N = 28$ shell closure for a better reproduction of the observed spectroscopic information on ^{56}Ni [39], and the probability of the inert $Z = N = 28$ closed core configuration in the ground state is found to be about 70% [40]. Thus, it is evident that, for a proper description of the experimental results for ^{62}Ni obtained in the present investigation, there is need to carry out shell model calculations using the entire fp model space, with use of an effective interaction which allows the simultaneous excitation of both protons and neutrons from the $1f_{7/2}$ orbitals.

Large-scale shell model calculations have thus been performed using a $^{40}_{20}\mathrm{Ca}_{20}$ core and the full fp model space for both protons and neutrons. The configuration space was truncated to allow up to four proton and six neutron excitations from the

$1f_{7/2}$ orbital to the upper fp shell. An effective interaction, called "GXPF1A" [41], which was especially designed for use in the full fp basis, has been used. The computer code NuShellX [42] has been used for the calculation of excitation energies and E2 and M1 transition strengths for the positive parity states with spins 0 to 6. The commonly used effective charges of $e_p = 1.5\,e$ for protons and $e_n = 0.5\,e$ for neutrons were employed to calculate B(E2)'s. For the calculation of B(M1)'s, the value of free g factors used for protons and neutrons are $g_p^s = +5.586$, $g_n^s = -3.826$, $g_p^l = +1$, and $g_n^l = 0$. The experimental and calculated level spectra for the positive parity states are compared in Fig. 5. It can be seen that the level density is satisfactorily reproduced by the calculation. Interestingly, the experimental excitation energies of the tentatively assigned (3_2^+) state and newly found 0_4^+ state are also nicely reproduced in the calculation. For the test of the quality of the wave functions of the underlying states obtained from the present shell model calculations, comparison between experimental and theoretical results for E2 and M1 decay rates have been presented in Table III. For most of the cases, the comparison is rewarding. It is interesting to see that the experimental B(E2) values have been reproduced well in the present shell model calculation with commonly accepted values of the effective charges. This success points to the fact that the truncation made in not allowing more than four protons and six neutrons from the respective π, $\nu(1f_{7/2})$ orbitals is not severe and also justifies the importance claimed for the $^{56}_{28}$Ni$_{28}$ core excitation.

Figure 6 demonstrates the calculated occupation numbers for the protons and neutrons of the fp orbitals in the relevant low-lying states in ^{62}Ni. It is seen from the figure that the $\nu(1f_{7/2})$ orbital remains almost closed. On the average, a single-proton excitation occurs from the $\pi(1f_{7/2})$ orbital for all the states. It is observed that the excitation of this single proton from the ^{56}Ni core has a significant impact on the transition rates. The wave functions

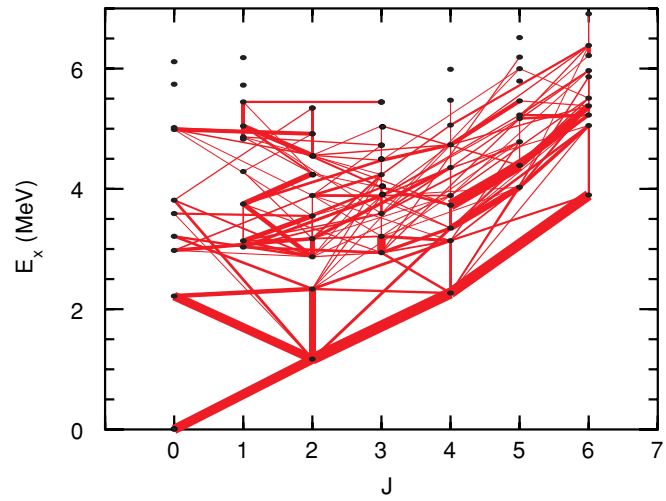

FIG. 7. (Color online) Levels in ^{62}Ni connected by bars whose widths are proportional to the calculated B(E2) values obtained in the present shell model calculation. Only those transitions which decay with a B(E2) value larger than 1 W.u. are depicted in the figure.

of the ground and excited states are found to be highly configuration mixed. The most dominant configuration for the ground 0^+ state is $\pi, \nu[(1f_{7/2})^{16}(2p_{3/2}, 1f_{5/2}, 2p_{1/2})^6]$ with a probability of 50%. The other dominant configurations are $\pi, \nu[(1f_{7/2})^{15}(2p_{3/2}, 1f_{5/2}, 2p_{1/2})^7]$ and $\pi, \nu[(1f_{7/2})^{14}(2p_{3/2}, 1f_{5/2}, 2p_{1/2})^8]$ with the respective probabilities of 26% and 12%.

It has thus been shown that the observed properties of the low-lying states of ^{62}Ni can be explained fairly well, except for the anomalously large $B(\mathrm{E2}; 0_2^+ \rightarrow 2_1^+)$ strength, by large-scale shell model calculations using the full fp model space. Proton excitations across the $Z = 28$ gap play an important role in reproducing the observed level structure. Breaking of the ^{56}Ni core is quite evident, even in the ground state of ^{62}Ni.

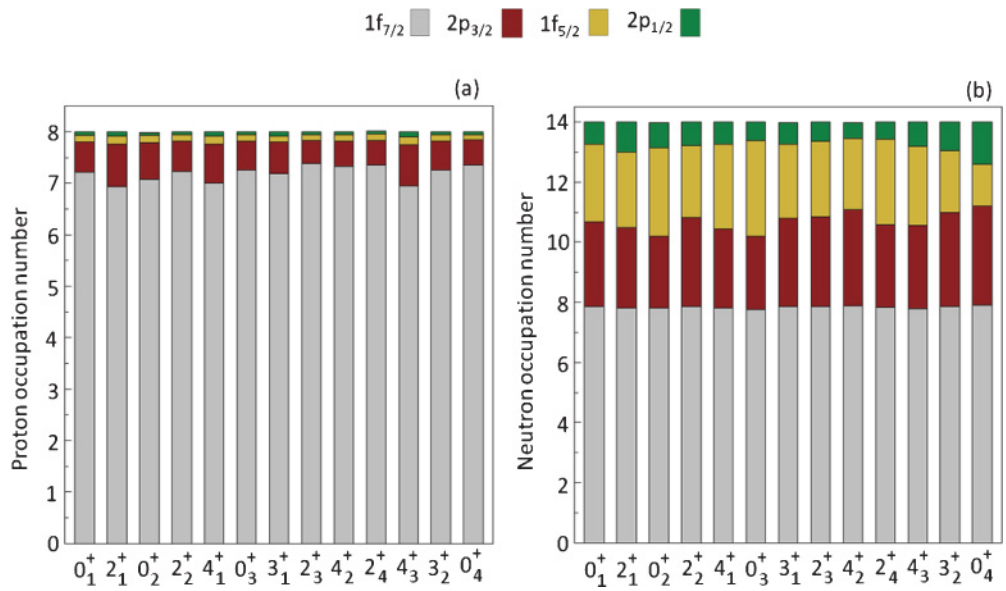

FIG. 6. (Color online) Calculated occupation numbers of the fp orbitals for the (a) protons and (b) neutrons in ^{62}Ni.

Complete mapping of the E2 strength for all the possible transitions connecting the low-spin states in ^{62}Ni, following shell model calculation, are shown in Fig. 7. The figure exhibits enhanced $B(E2)$ values for the transitions from the 0^+, 2^+, and 4^+ two-phonon states, near 2.2 MeV, to the first 2^+ state. It is obvious from the figure that no states, except for the 6^+ near 3.9 MeV, decay to the two-phonon states with enhanced E2 strength. This points toward the fact that there is loss of collectivity and subsequent breakdown of multiphonon structure at higher excitation ($E_x > 2.3$ MeV).

V. CONCLUSIONS

Lifetimes of the states up to $E_x = 3.7$ MeV have been measured through the DSAM technique with the ^{62}Ni$(n,n'\gamma)$ reaction. Mean lifetime values obtained in this work are in good agreement with the values listed in the latest compilation [30] for most of the states, although deviations have been observed in a few cases. Lifetime information for previously unmeasured and newly discovered levels have also been provided. Additional measurements are required to obtain the lifetime of the 0_2^+ state with greater accuracy. While there is some evidence for two-phonon states, the data clearly do not support the existence of higher-phonon states. Excitation of protons across the $Z = 28$ shell closure is found to be an essential feature in understanding the observed level structure and transition rates.

ACKNOWLEDGMENTS

The authors are indebted to H. E. Baber for his expert assistance in providing the excellent proton beams during the experiments. One of the authors (A.C.) would like to thank the governing authority of Krishnath College, Berhampore, West Bengal, India, for granting a leave to carry out this research. This material is based upon work supported by the U.S. National Science Foundation under Grant Nos. PHY-0956310 and PHY-0758099.

[1] S. Cohen, R. D. Lawson, M. H. Macfarlane, S. P. Pandya, and M. Soga, Phys. Rev. **160**, 903 (1967).
[2] N. Auerbach, Phys. Rev. **163**, 1203 (1967).
[3] P. W. M. Glaudemans, M. J. A. de Voigt, and E. F. M. Steffens, Nucl. Phys. A **198**, 609 (1972).
[4] O. Kenn, K.-H. Speidel, R. Ernst, J. Gerber, P. Maier-Komor, and F. Nowacki, Phys. Rev. C **63**, 064306 (2001).
[5] C. Vaman *et al.*, Phys. Rev. Lett. **99**, 162501 (2007).
[6] J. N. Orce, B. Crider, S. Mukhopadhyay, E. Peters, E. Elhami, M. Scheck, B. Singh, M. T. McEllistrem, and S. W. Yates, Phys. Rev. C **77**, 064301 (2008).
[7] N. J. Stone, At. Data Nucl. Data Tables **90**, 75 (2005).
[8] J. M. G. Gomez, Phys. Rev. C **6**, 149 (1972).
[9] T. E. Ward, P. H. Pile, and P. K. Kuroda, J. Inorg. Nucl. Chem. **31**, 3023 (1969).
[10] H. W. Jongsma, J. C. de Lange, J. C. Boddendijk, R. Kamermans, and H. Verheul, Nucl. Phys. A **150**, 520 (1970).
[11] A. Boucenna, L. Kraus, I. Linck, and T. U. Chan, Phys. Rev. C **42**, 1297 (1990).
[12] N. Stein, J. W. Sunier, and C. W. Woods, Phys. Rev. Lett. **38**, 587 (1977).
[13] O. Karban, A. K. Basak, F. Entezami, and S. Roman, Nucl. Phys. A **366**, 68 (1981).
[14] E. K. Warburton, J. W. Olness, A. M. Nathan, and A. R. Poletti, Phys. Rev. C **18**, 1637 (1978).
[15] K. Itoh, M. Oyamada, and Y. Torizuka, Phys. Rev. C **7**, 458 (1973).
[16] D. M. Van Patter, E. J. Hoffman, T. Becker, and P. A. Assimakopoulos, Nucl. Phys. A **178**, 355 (1972).
[17] Yu. G. Kosyak, D. K. Kaipov, and L. V. Chekushina, Izv. Akad. Nauk SSSR, Ser. Fiz. **53**, 2130 (1989) [Bull. Acad. Sci. USSR, Phys. Ser. **53**, 68 (1989)].
[18] I. Kumabe, M. Matoba, M. Inoue, S. Matsuki, and E. Takasaki, Bull. Inst. Chem. Res., Kyoto Univ. **60**, 106 (1982).
[19] H. Junde and B. Singh, Nucl. Data Sheets **91**, 317 (2000).
[20] P. E. Garrett, K. L. Green, and J. L. Wood, Phys. Rev. C **78**, 044307 (2008).
[21] P. E. Garrett and J. L. Wood, J. Phys. G **37**, 064028 (2010).
[22] P. E. Garrett, N. Warr, and S. W. Yates, J. Res. Natl. Inst. Stand. Technol. **105**, 141 (2000).
[23] S. W. Yates, J. Radioanal. Nucl. Chem. **265**, 291 (2005).
[24] M. Scheck, S. N. Choudry, E. Elhami, M. T. McEllistrem, S. Mukhopadhyay, J. N. Orce, and S. W. Yates, Phys. Rev. C **78**, 034302 (2008).
[25] J. Theuerkauf, S. Esser, S. Krink, M. Luig, N. Nicolay, O. Stuch, and H. Wolters, computer code Tv, 1993, [http://www.ikp.uni-koeln.de/~fitz].
[26] T. Belgya, G. Molnár, and S. W. Yates, Nucl. Phys. A **607**, 43 (1996).
[27] K. B. Winterbon, Nucl. Phys. A **246**, 293 (1975).
[28] E. Sheldon and V. C. Rogers, Comput. Phys. Commun. **6**, 99 (1973); P. A. Moldauer, Phys. Rev. C **14**, 764 (1976).
[29] J. F. Ziegler, *Handbook of Stopping Cross-Sections for Energetic Ions in All Elements* (Pergamon, New York, 1980).
[30] ENSDF database: [www.nndc.bnl.gov/ensdf/].
[31] S. Raman, C. W. Nestor Jr., and P. Tikkanen, At. Data Nucl. Data Tables **78**, 1 (2001).
[32] D. L. Kennedy, H. H. Bolotin, I. Morrison, and K. Amos, Nucl. Phys. A **308**, 14 (1978).
[33] A. Passoja, R. Julin, J. Kantele, and M. Luontama, Nucl. Phys. A **363**, 399 (1981).
[34] U. Fanger, D. Heck, W. Michaelis, H. Ottmar, H. Schmidt, and R. Gaeta, Nucl. Phys. A **146**, 549 (1970).
[35] H. Ohnuma, J. Kasagi, Y. Iritani, and N. Kishida, J. Phys. Soc. Jpn. **45**, 1092 (1978).
[36] D. H. Kong-A-Siou and H. Nann, Phys. Rev. C **11**, 1681 (1975).
[37] S. R. Lesher *et al.*, Phys. Rev. C **76**, 034318 (2007).
[38] E. Sheldon and D. M. van Patter, Rev. Mod. Phys. **38**, 143 (1966).
[39] M. Horoi, B. A. Brown, T. Otsuka, M. Honma, and T. Mizusaki, Phys. Rev. C **73**, 061305(R) (2006).
[40] M. Honma, T. Otsuka, B. A. Brown, and T. Mizusaki, Phys. Rev. C **65**, 061301(R) (2002).
[41] M. Honma, T. Otsuka, B. A. Brown, and T. Mizusaki, Eur. Phys. J. A **1**, 499 (2005).
[42] Computer code NUSHELLX@MSU, by B. A. Brown, W. D. M. Rae, E. McDonald, and M. Horoi, [http://www.nscl.msu.edu/~brown/resources/resources.html].